International Journal of Nanomedicine

Dovepress
Taylor & Francis Group

Open Access Full Text Article

ORIGINAL RESEARCH

Intramuscular All-Trans Retinoic Acid-Adjuvanted Nanovaccine Elicits Robust Mucosal and Systemic Immunity Against *Helicobacter pylori*

Junhua Xu, Min Sun, Ning Wang, Yun Shi, Yu Liu, Runqing Tan, Song Zhou, Gang Guo, Kaiyun Liu

Institute of Biopharmaceuticals, West China Hospital, Sichuan University, Chengdu, 610041, People's Republic of China

Correspondence: Kaiyun Liu; Gang Guo, Email liukaiyun@wchscu.edu.cn; guogang7001@163.com

Purpose: *Helicobacter pylori* (*H. pylori*) infection, implicated in chronic gastritis, peptic ulcers, and gastric cancer, poses a significant global health burden exacerbated by increasing antibiotic resistance. Traditional intramuscular vaccines often yield limited mucosal immunity, necessitating the development of more effective vaccination strategies capable of robust mucosal and systemic responses. Here, we report a novel nanovaccine (RA-NVs) combining all-trans retinoic acid (RA) and recombinant urease subunit proteins (UreA/UreB), encapsulated in poly(lactic-co-glycolic acid) (PLGA) nanoparticles to enhance protective immunity against *H. pylori*.

Methods: RA-NVs were synthesized via single emulsion–diffusion–evaporation, with antigens loaded onto the nanoparticle surfaces. Their physicochemical properties, antigen loading capacity, and stability were characterized. In vitro dendritic cell (DC) activation, antigen uptake, and gut-homing receptor expression (C-C chemokine receptor 9, CCR9) were assessed. In vivo distribution was examined using in vivo imaging system (IVIS). BALB/c mice were immunized intramuscularly, and subsequent mucosal (IgA) and systemic (IgG) antibody responses, cytokine profiles, T cell proliferation, and bacterial clearance upon *H. pylori* challenge were evaluated. Vaccine biosafety was assessed via histopathological and biochemical analyses.

Results: RA-NVs exhibited optimal size, surface charge, and sustained antigen and RA release. In vitro assays demonstrated efficient DC uptake, enhanced CCR9 expression, cytokine secretion (IL-6, IL-10, IL-15), and improved DC migration towards C-C motif chemokine ligand 25 (CCL25). In vivo, RA-NVs significantly elevated serum IgG and mucosal IgA antibodies, promoted CD4+ and CD8+ T cell activation, and elicited robust Th2/Th17-skewed responses. Notably, immunized mice exhibited significantly reduced gastric bacterial colonization and inflammation upon *H. pylori* challenge, alongside excellent safety profiles with minimal toxicity and organ damage.

Conclusion: The RA-adjuvanted nanovaccine effectively induces potent mucosal and systemic immunity via intramuscular administration, representing a promising strategy against mucosal pathogens such as *H. pylori*. This nanovaccine platform addresses key limitations associated with oral vaccination and with conventional intramuscular approaches that often yield limited mucosal immunity, offering an alternative for enhancing mucosal vaccine efficacy in mice; although a direct head-to-head comparison with an oral formulation remains to be established.

Plain Language Summary: Helicobacter pylori (*H. pylori*) is a bacterium that infects the stomach lining and can lead to serious health issues, including ulcers and even stomach cancer. Antibiotics have been used to treat this infection, but they are becoming less effective due to growing antibiotic resistance. A vaccine that triggers a strong immune response in both the blood and the gut could provide better protection.

In this study, our research team designed a new vaccine called RA-NVs. It is made of nanoparticles containing vitamin A derivative (retinoic acid) and two antigens from *H. pylori*. Unlike traditional vaccines, these nanoparticles help immune cells find their way specifically to the gut, the main site where the bacteria cause damage.

When we tested this vaccine in mice, we found it effectively activated the immune system, producing antibodies that protect the stomach lining. Mice that received our vaccine had significantly fewer bacteria in their stomachs after exposure to *H. pylori* and showed much less stomach inflammation. We also confirmed that the vaccine is safe and did not harm vital organs.

Received: 30 July 2025
Accepted: 13 December 2025
Published: 28 December 2025

Our results suggest this new vaccine is a promising tool to prevent stomach infections caused by *H. pylori*. This approach might also be useful for developing vaccines against other infections that affect mucosal surfaces, like those in the gut or respiratory tract.

Keywords: Helicobacter pylori, nanovaccine, all-trans retinoic acid, mucosal immunity, intramuscular delivery

Introduction

Mucosal infections, which affect the mucosae of the respiratory, oral, gastrointestinal, and genitourinary tracts, present significant global health challenges.[1,2] These infections often require localized immune responses at the sites of pathogen entry. To effectively prevent colonization and disease progression, vaccines must elicit robust local mucosal immunity.[3]

Among mucosal pathogens, *Helicobacter pylori* (*H. pylori*) is particularly notable for its ability to colonize the gastric mucosa, leading to chronic gastritis, peptic ulcers, and an increased risk of gastric cancer. It has been classified as a Group I carcinogen by the World Health Organization (WHO).[4] *H. pylori* infection affects more than half of the global population, with a particularly high prevalence in developing regions.[5] The effectiveness of current treatments relies on antibiotics in combination with proton pump inhibitor(PPI). However, the rise of antibiotic-resistant strains significantly compromises its effectiveness and also fails to offer long-term protection against reinfection.[6] This situation underscores the urgent need for effective vaccines capable of inducing mucosal immunity against *H. pylori*.[7]

Our research team has previously investigated *H. pylori* infection and vaccine development, with a focus on enhancing mucosal immunity. Previously, we focused on developing oral vaccines using protein-based antigens to directly target the GI tract, the natural site of *H. pylori* colonization.[8] While oral vaccines are ideal for delivering antigens to the GI tract, they are susceptible to several limitations, including degradation by gastric acid and digestive enzymes.[9] These barriers often result in reduced antigen effectiveness and, consequently, suboptimal immune responses. Recognizing these challenges, we aimed to develop a more robust approach that could overcome these limitations and provide more reliable protection against *H. pylori*.

A promising strategy to enhance mucosal immunity involves the use of all-trans retinoic acid (RA), a metabolite of vitamin A known for its immunomodulatory properties.[10,11] RA has been shown to upregulate gut-homing receptors such as CCR9 on immune cells,[12] which are critical for directing them to the gut-associated lymphoid tissues (GALTs) where mucosal immune responses are initiated. Previous studies have explored various methods of delivering RA in combination with antigens to enhance mucosal immunity.[13–17] For instance, complex delivery systems like oil-in-polymer capsules or separate delivery of RA and antigens to lymph nodes have been employed to stimulate immune responses.[13] However, these approaches often involve complicated manufacturing processes and require high doses of RA, raising concerns about potential toxicity and immune tolerance. Additionally, the scalability of these methods for widespread clinical use remains a significant challenge.[14,16]

Herein, we aim to develop and evaluate RA-NVs, a nanovaccine designed to elicit both systemic and mucosal immune responses against *H. pylori*. To address the aforementioned limitations, we formulated PLGA (poly(lactic-co-glycolic acid)) nanoparticles encapsulating RA, with their surfaces functionalized with two recombinant *H. pylori* antigens, UreA and UreB. These antigens are considered promising vaccine candidates due to their essential role in the bacterial urease enzyme, a key virulence factor critical for gastric colonization and acid resistance.[18,19]

This strategy offers several distinct advantages over previous methods. First, compared with alternative biodegradable systems (eg, chitosan/alginate or polyanhydrides), PLGA offers a pragmatic balance of established safety, antigen/adjuvant compatibility, and manufacturability for the present intramuscular design. PLGA nanoparticles facilitate efficient uptake by antigen-presenting cells, thereby enhancing immune responses. In addition, their widely documented controlled-release behavior can support sustained delivery of all-trans retinoic acid (RA), which may help reduce the required dose and mitigate risks related to toxicity or tolerance. Furthermore, by upregulating CCR9 expression on immune cells, this formulation promotes gut-homing and facilitates both systemic and mucosal immunity (Scheme 1). Unlike our previous oral vaccine formulations, intramuscular administration of RA-NVs avoids degradation by gastric acid and enzymes, ensuring more consistent antigen delivery and robust immune activation. In this study, we focus on

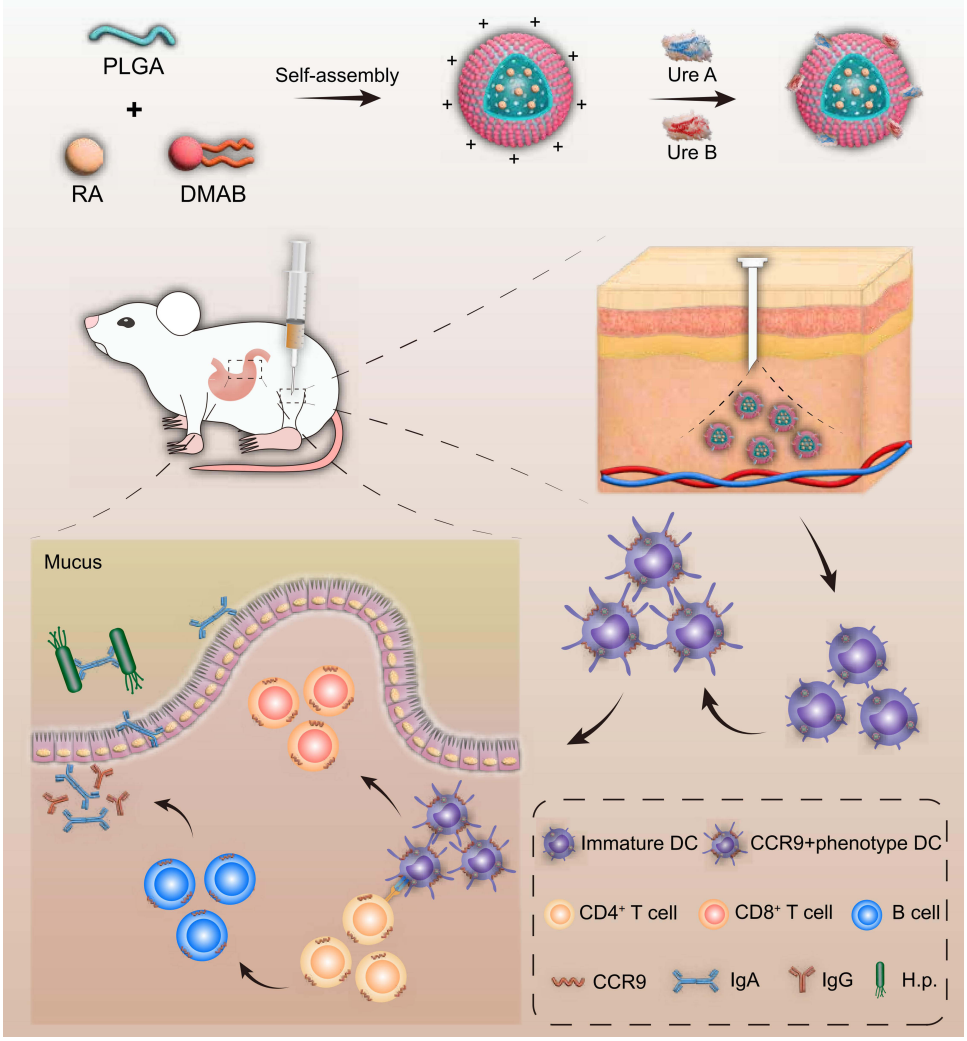

Scheme 1 Schematic representation of the RA-NVs nanovaccine and its immune response mechanism.
Notes: The nanovaccine is formulated by self-assembly of PLGA, retinoic acid, and DMAB. UreA and UreB antigens are adsorbed onto the surface to create the nanovaccine (RA-NVs). Following intramuscular injection, the nanovaccine forms an antigen depot at the injection site, allowing for sustained antigen release. Dendritic cells (DCs) take up the nanovaccine and mature, priming both CD4+ and CD8+ T cells. This induces systemic immunity with IgG production and mucosal immunity through sIgA secretion, targeting *H. pylori* colonizing the gastric mucosa.

assessing the immunogenicity, protective efficacy, and biosafety of this nanovaccine, with the goal of advancing vaccine strategies for mucosal bacterial infections.

Materials and Methods

Materials

PLGA acid terminated (50/50 lactide/glycolide copolymer), Didodecyldimethylammonium bromide (DMAB) and polyvinyl alcohol (PVA; MW 30–70 kDa) was purchased from Adamas Reagent Co. (Shanghai, China). All trans-retioinic acid (RA) and ovalbumin (OVA) were purchased from Sigma Aldrich (Shanghai, China). Cyanine5 (Cy5) N-hydroxysuccinimide ester (Cy5-NHS) were purchased from Duofluo (Wuhan, China). Other reagents were purchased from Sangon (Shanghai, China) unless noted specifically.

Antigen, Cells, Bacterial Strains, and Animals

The genes encoding urease subunit A (UreA) and urease subunit B (UreB) were synthesized and cloned into the pET28a (+) and pET22b(+) plasmids, respectively (GeneCreate Biotechnology Company, Wuhan, China). The recombinant

https://doi.org/10.2147/IJN.S557242

plasmids were transformed into *Escherichia coli* BL21(DE3) for protein expression. Recombinant UreA and UreB proteins were expressed in *E. coli*, and their purity (>95%) was confirmed using HPLC.

Female BALB/c mice (4–6 weeks old) were purchased from Dossy Experimental Animals Co., Ltd. (Chengdu, China). They were housed in sterile cages of five animals or less with a 12 h light/12 h dark schedule, which were equipped with laminar airflow hoods in a specific pathogen-free room. And autoclaved chow and water ad libitum were employed to feed all the animals. Collectively, mice were guaranteed with at least one-week acclimation before the experiments.

The *H. pylori* J99 strain (ATCC700824) was purchased from the American Type Culture Collection and adapted for colonization in gastric mucosa of BALB/c mice through a series of passages comprising five isolation-reinfection cycles in vivo. The mouse-adapted strain was cultured in optimized Skirrow broth[20] for 24 hours and then harvested for mouse infection in this study.

Preparation and Characterization of Nanovaccines

RA-loaded nanovaccines (RA-NVs) were prepared using single emulsion–diffusion–evaporation method as previously reported.[21] In brief, 2.5 mL of acetone and ethanol mixture (v/v=4/1) containing 50 mg of (PLGA), 5 mg of DMAB, and varying amounts of RA was injected into 15 mL of F-127 (0.5%, w/v) and PVA (0.5%, w/v) solution via a syringe pump and then was put under stirring to solidify for 24 h. The particles were washed by centrifugation with distilled water and were further freeze-dried. *H. pylori* antigen UreA and UreB (2mg/mL each) were loaded onto the nanoparticles by mixing and stirring for 4 hours at 4 °C to obtain the RA-NVs. Then the mixture was washed by centrifugation to remove unloaded antigen. The morphology of nanovaccines was examined on a transmission electron microscope (JEM 2100Plus, Japan) at an acceleration voltage of 200 kV. The particle size distribution and zeta potential were measured using a Zeta-sizer (Malvern Instruments, UK) at 25 °C. The concentration of RA was determined by HPLC and UreA and UreB was determined by SDS-PAGE as previously reported.[22]

In vitro Cytotoxicity Evaluation

Mouse bone marrow-derived dendritic cells (BMDCs)were isolated and cultured following established protocols.[23] Then the DC cells were seeded into a 96-well culture plate (10^4 cells/well) and allowed to adhere and grow for 72h. Various formulations were then added at concentrations ranging from 10 to 200 μg/mL. Following a 24-hour incubation period, cell viability was measured using the cell counting kit-8 (CCK-8) assay. A microplate reader (BioTek Synergy H1) was used to evaluate the colorimetric density at 450 nm.

In vitro BMDCs Uptake and Cytokine Assays

Ovalbumin (OVA), used as a model antigen, was tagged with Cy5-NHS according to the manufacturer's instructions before being loaded on RA-NVs. After incubation with various formulations for 4 hours, BMDCs were stained with Lysotracker and Hoechst 33342. Images were obtained by a laser confocal fluorescence microscope (Nikon, Japan). In all experimental groups, OVA and RA were kept consistent.

To evaluate the activation of BMDCs, the cells were treated with different formulations as described above for 24 h. The cells were stained with Fixable Viability Stain 700, BV421 Hamster Anti-Mouse CD11c (HL3), and PE anti-mouse CD199 (CCR9) and analyzed by flow cytometry using the LSRFortessa system (BD Biosciences, USA).

Transwell Migration Assay

A Transwell model was employed to simulate the extracellular matrix (ECM) within gastrointestinal tissues and to evaluate the migratory capacity of dendritic cells (DCs).[24,25] The apical compartment of Transwell plate (24-well, 5-μm pore size), was pre-coated with Matrigel® according to manufacturer's protocol. The receiver compartment was supplemented with CCL25 (2 μg/mL) and BMDC (5×10^5 cells/well). After BMDCs were incubated with the following formulations, including PBS, RA+antigens, NVs, and RA-NVs for 48 hours, the cells were collected and seeded at concentration of 5×10^5/well in both the apical and receiver compartment. After 12 hours, the cells in the receiver

compartment were collected and counted using a hemocytometer. The migration efficiency of DCs was calculated using the formula: Migration Efficiency of DCs (%) = (Cell Number in Receiver Compartment/5 × 10^5) *100%.

IVIS Imaging

To visualize the in vivo distribution of the nanovaccine after intramuscular injection into the thigh region of mice, Cy5-OVA@RA-NVs and Cy5-OVA solutions (OVA 1 mg/mL, 50 μL) were administered to the mice. The animals were randomly divided into two groups (n = 2 per group). At predetermined time points, the mice were imaged using an in vivo imaging system (IVIS, PerkinElmer).

Serum IgG and Mucosal IgA Assay

Female BALB/c mice aged 6–8 weeks were randomly assigned into four groups (12 animals per group). Various formulations including antigen and RA mixed solution, NVs, and RA-NVs containing 18 μg of UreA, 24 μg of UreB, and 40 μg of RA were intramuscularly primed on day 1 and boosted on days 14, and 21. Blood samples were collected on day 28. Vaginal lavage fluids(VLF) were collected at day 35 and day42. Serum was diluted 1:200. VLFs were diluted at 1:5. Levels of IgG in serum and IgA in VLFs were measured using standard ELISA protocol.

Cellular Immune Responses Assay

On day 35 and 42 post immunization, spleens and Peyer's patch were harvested and grinded to obtain single-cell suspension. The isolated splenocytes were cultured at density of 10^6 cells /well. The splenocytes were stimulated with nanovaccines containing 10 μg/mL of antigen and incubated for 72 h. Then the supernatant of cultured cells was collected. The levels of IL-4, IFN- γ, and IL-17 in supernatant were quantified with an ELISA kit (R&D Systems, USA) according to the manufacturer's instructions. The splenocytes were stimulated using nanovaccines containing 10 μg/mL of antigen and concanavalin A(ConA) for 72 h to induce splenocyte growth. Cell proliferation was then evaluated using the Cell Counting Kit-8 (BBI, China).

On day 35 and 42 post immunization, Peyer's patch from each mouse were harvested and grinded to obtain single-cell suspension. Then the cells were collected by centrifugation and stained with a panel of fluorescent antibodies, including V500-Anti-Mouse CD45, PerCP-Cy5.5-Anti-Mouse CD19, FITC-Anti-Mouse CD45R/B220, BV421-Anti-Mouse CD138, Fixable Viability Stain 700 (all from BD Biosciences). The cells were washed with PBS and analyzed by flow cytometry using the LSRFortessa system (BD Biosciences, USA).

Histopathological Analysis of Major Organs

After 42 days post-immunization, the immunized mice were sacrificed, and their major organs, including the heart, liver, spleen, lungs, and kidneys, were collected. The organs were fixed in 4% paraformaldehyde and then processed for histopathological analysis. The tissue samples were embedded in paraffin, sectioned into 3 μm slices, and stained with hematoxylin and eosin (H&E).

Immunogenicity and Protective Efficacy

Female BALB/c mice aged 6–8 weeks were randomly assigned into four groups (10 per group). Various formulations including antigen and RA mixed solution, NVs, and RA-NVs containing 18 μg of UreA, 24 μg of UreB, and 40 μg of RA were intramuscularly primed on day 1 and boosted on days 14, and 21. On day 35, mice were fasted overnight. On the following day, 7.5% $NaHCO_3$ was administered to the mice by oral gavage to neutralize gastric acid, followed by 0.2 mL of H. pylori J99 suspension (4×108 CFU) via the same route. On day 49, the animals were euthanized and the number of bacteria in the stomach was quantified by a quantitative culture method.[26] The gastric biopsies were embedded in paraffin, sectioned into 3 μm slices, and stained with H&E.

Serum Biochemical Parameters

On day 35, serum samples were collected from the immunized mice. Biochemical parameters, including Alkaline phosphatase (ALP2L), Alanine transaminase (ALTL), Aspartate Transaminase (ASTL), Creatine Kinase (CK), lactate

dehydrogenase (LDHI2), uric acid (UA2), Ureal, Creatinine (CREA2) were analyzed using an automated clinical chemistry analyzer (Cobas C702, Roche, US).

Statistics

All animal studies were performed with randomization. All data are presented as means ± s.e.m. Statistical significance was determined with a one-way analysis of variance (ANOVA) followed by Tukey's multiple comparison test for multiple group comparisons. A p-value of less than 0.05 was considered statistically significant. All statistical analyses were conducted using GraphPad Prism software, version 9.

Results and Discussion

Characteristics of RA-NVs

The physicochemical characterization of antigen- and RA- loaded nanovaccines (RA-NVs) was first conducted to validate their successful formulation. Prior to antigen loading, the expression and purity of both UreA and UreB antigen were confirmed by SDS-PAGE and Western Blot (Figure S1). Upon loading onto the nanocarriers, the antigen loading capacities were 7.2% for UreA and 9.6% for UreB. Transmission electron microscopy (TEM) images revealed that the nanovesicles exhibited a spherical morphology with uniform size distribution (Figure 1a). Dynamic light scattering (DLS) analysis demonstrated that both bare NVs and RA-NVs exhibited narrow size distributions, although RA-NVs showed a modest increase in hydrodynamic diameter due to surface adsorption of the antigens (Figure 1b).

The RA-NVs exhibited a negative zeta potential (Figure 1c), which is typical for PLGA-based nanocarriers. To facilitate antigen adsorption, DMAB was employed to provide positive charges on the surface.[27] Upon antigen loading, a slight reduction in zeta potential (+7.44 → +2.54 mV, [PBS, pH 7.4]) and modestly increased hydrodynamic diameter (~38 nm) was observed. These changes consistent with surface adsorption of negatively charged antigens but not definitive on their own. The colloidal stability of the NVs and RA-NVs was evaluated by monitoring the hydrodynamic diameters over a 28-day storage period (Figure 1d). Both formulations maintained their size without significant aggregation or degradation, indicating robust stability.

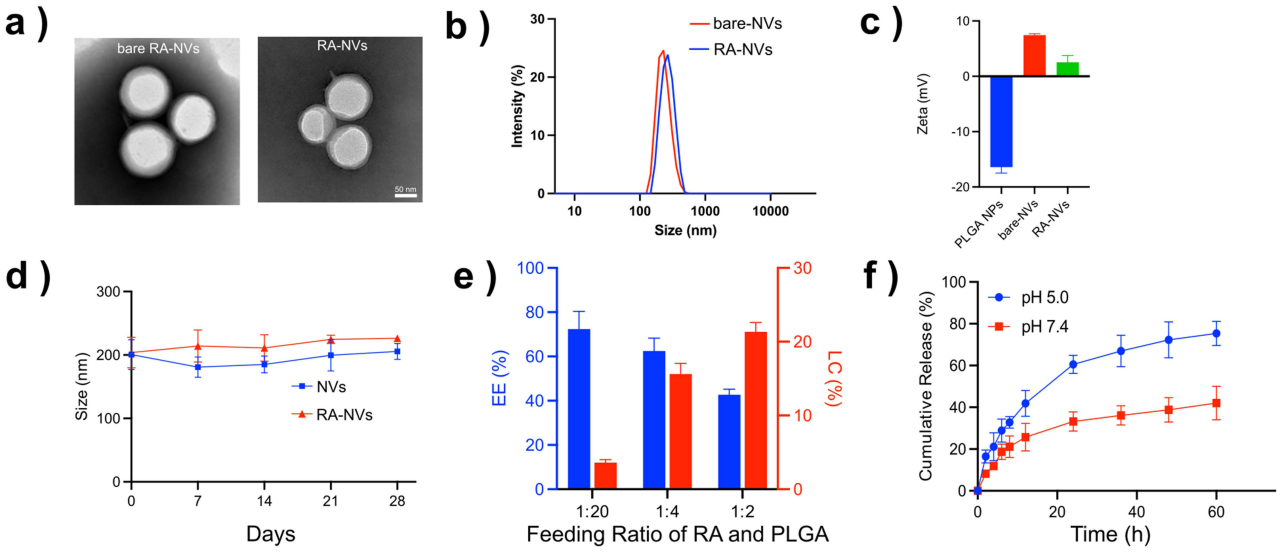

Figure 1 Physiocochemical characterization of NVs.

Notes: (**a**) Representative TEM image of bare RA-NVs (Left) and RA-NVs (Right). Scale bar: 50 nm. (**b**) Hydrodynamic size distribution and (**c**) zeta potentials of various formulations. (**d**) Hydrodynamic diameters of NVs and RA-NVs after storage for 28 days. (**e**) Encapsulation efficiency (EE) and loading capacity of RA at various feeding ration of RA and PLGA. (**f**) In vitro release profile of RA at various pH values. Data are shown as mean±SD (standard deviation). n=3 technical replicates.

Encapsulation efficiency (EE) and loading capacity (LC) of RA were evaluated at different RA-to-PLGA feeding ratios (Figure 1e). An optimal mass ratio of 1:4 (RA:PLGA) was selected for subsequent studies based on maximized drug loading performance.

The in vitro release profile of RA was assessed under acidic conditions (pH 5.5) mimicking the lysosomal microenvironment (Figure 1f). The RA-NVs exhibited sustained release behavior under these conditions, supporting their potential for intracellular drug delivery following endocytic uptake.

Antigen Uptake and Activation by BMDCs in Vitro

Biocompatibility of RA-NVs was evaluated using a cell viability assay with bone marrow-derived dendritic cells (BMDCs). As shown in Figure 2a, BMDCs maintained high viability across all concentrations of NVs and RA-NVs, confirming their non-toxicity and suitability for in vivo applications. Confocal microscopy further demonstrated

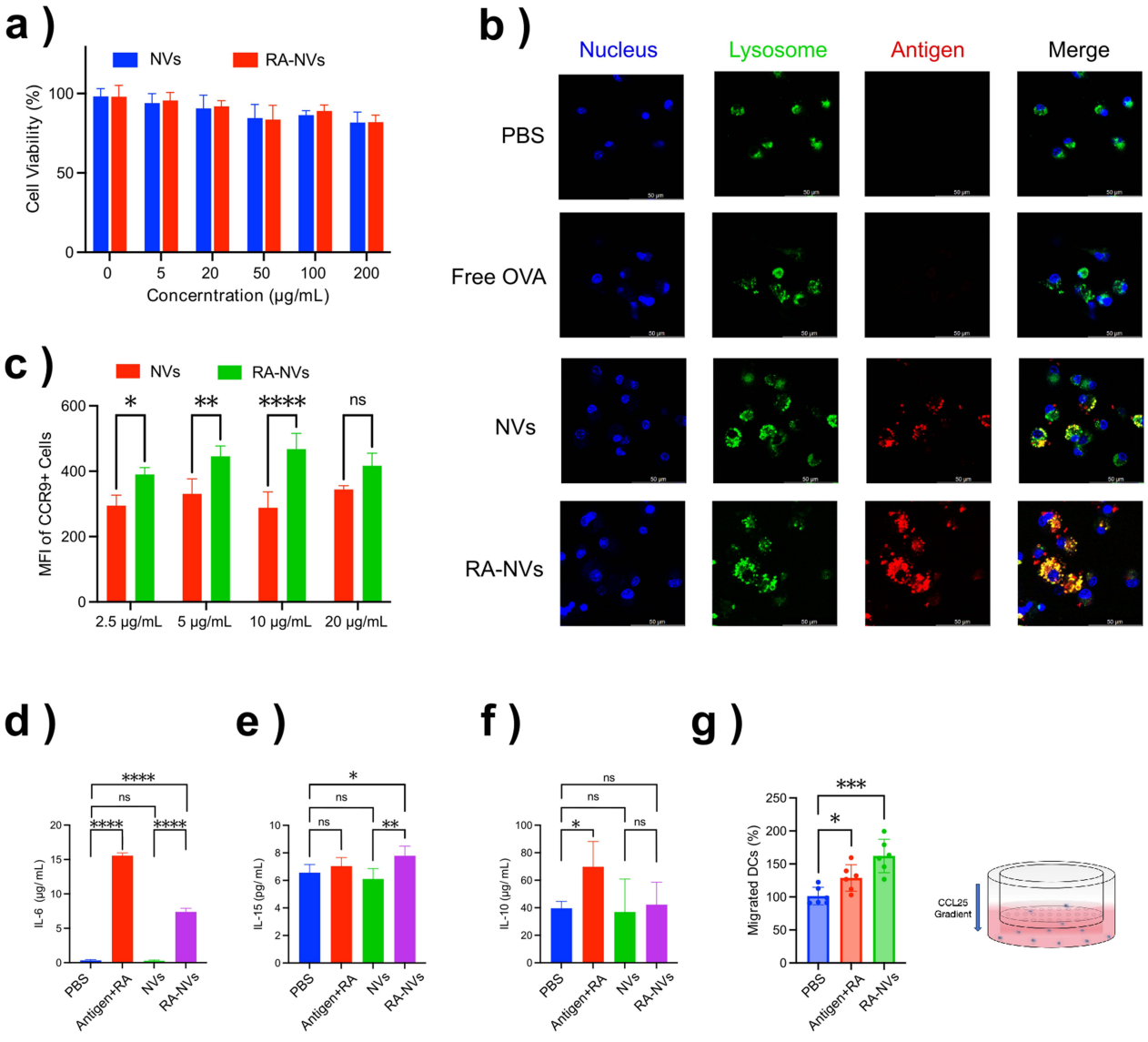

Figure 2 (**a**) Cell viability assay by cell exposed to different amount of NVs and RA-NVs. (**b**) Representative confocal microscopy images of internalization and intracellular localization of various formulation on BMDC. Scale bar: 50 μm. (**c**) The expression of CCR9 were quantified by flow cytometry. (**d**) IL-6, (**e**) IL-15, and (**f**) IL-10 concentration in supernatants of BMDCs using ELISA kits. (**g**) Schematic illustration of an in vitro Transwell model (right) showing DC migration in gut-homing-environment. (**d–f**). One-way ANOVA with Dunnett's test (each group vs PBS); pre-specified comparison RA-NVs vs NVs is also shown. (**g**) One-way ANOVA with Dunnett (vs PBS); pre-specified comparison RA-NVs vs Antigen+RA shown. Data are shown as mean±SD. n=6. ns, not significant, *p < 0.05, **p < 0.01, ***p < 0.001, ****p < 0.0001.

https://doi.org/10.2147/IJN.S557242

extensive cellular uptake and lysosomal colocalization of Cy5-labeled ovalbumin (OVA) when delivered via OVA@NVs and OVA@RA-NVs, compared to free OVA (Figure 2b), suggesting efficient endocytosis and subsequent intracellular trafficking where the pH-sensitive release of RA likely occurs. Quantitative colocalization analysis (Pearson's correlation and Manders' coefficients) confirmed stronger antigen–lysosome overlap for OVA@NVs than for OVA@RA-NVs (Figure S2), consistent with reduced lysosomal sequestration of antigen in the RA-NV group.

Flow cytometry analysis revealed a significant upregulation of the gut-homing receptor CCR9 on BMDCs after treatment with RA-NVs at 10 μg/mL (Figure 2c), consistent with previous reports demonstrating the ability of RA to imprint gut-homing specificity on immune cells.[12] However, increasing the dose to 20 μg/mL did not further enhance CCR9 expression, potentially due to cell stress, although no cytotoxicity was observed.[28] These results support the selection of 10 μg/mL as the optimal concentration.

To investigate their immunomodulatory properties, cytokines were quantified in BMDC culture supernatants after treatment (Figures 2d–f). RA-NVs significantly increased the production of IL-6, IL-15, and IL-10 compared to controls. IL-6 and IL-15 are associated with T-cell activation and proliferation, while IL-10 supports immune regulation and mucosal tolerance. These findings indicate that RA-NVs promote an immunological environment conducive to both innate and adaptive responses.

To further explore the impact of RA-NVs on immune cell migration, an in vitro Transwell migration assay was conducted to simulate the gut-homing environment (Figure 2g). Treatment with RA-NVs significantly enhanced DC migration toward CCL25, consistent with CCR9 upregulation, which is known to direct immune cells to gut-associated lymphoid tissues.[29,30] These results suggest that RA-NVs not only imprint a gut-homing phenotype on dendritic cells but may also direct their migration toward gastrointestinal lymphoid tissues.

Distribution and Retention of RA-NVs in vivo

To evaluate antigen distribution and retention in vivo, Cy5-labeled ovalbumin (Cy5-OVA) encapsulated in RA-NVs was intramuscularly injected, and monitored using an IVIS imaging system. As shown in Figures 3a and b, a clear antigen depot was formed at the injection site. The fluorescent signals from Cy5-OVA@RA-NVs were significantly stronger and persisted longer compared to the free Cy5-OVA group, indicating efficient local retention of the nanovaccine. Such sustained antigen availability at the injection site is critical for prolonged antigen exposure to immune cells, potentially enhancing immunogenicity and providing durable immune responses.

Systemic and Mucosal Immune Responses

The immune responses induced by RA-NVs were evaluated in BALB/c mice following intramuscular vaccination, with systemic and mucosal immune responses measured at specified intervals (Figure 4a and Table S1). On Day 28, serum IgG titers for both UreA and UreB antigens were significantly elevated in the RA-NVs group compared to the antigen + RA and NVs groups (Figure 4b). In addition, RA-NVs elicited significantly elevated antigen-specific IgA levels in vaginal lavage fluid (VLF) on Day 35 compared to controls (Figure 4c), indicating effective mucosal priming. Vaginal IgA levels were further evaluated on Day 42 (Figure S3). UreA-specific IgA levels remained significantly elevated in the RA-NVs group, indicating a sustained mucosal response, while UreB-specific IgA levels showed no significant difference between groups at this time point. Direct gastric-site assays were not performed in this proof-of-concept

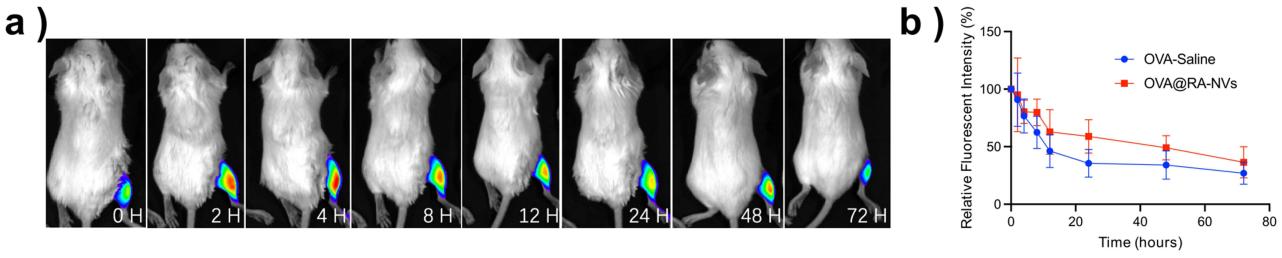

Figure 3 (**a**) IVIS images of mice receiving intramuscular injection of Cy5-OVA@RA-NVs. (**b**) Quantification of fluorescent signals of mice over time.

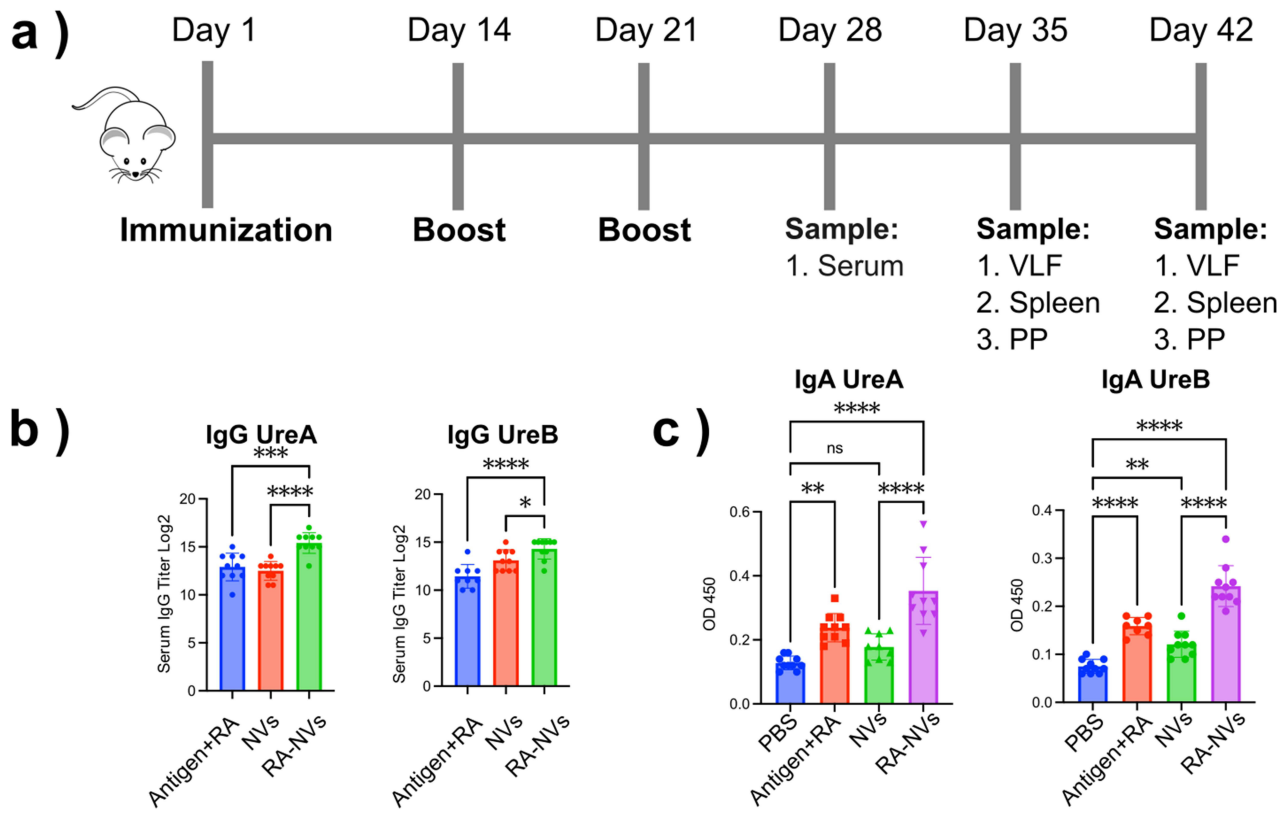

Figure 4 (**a**) Scheme of experiment. BALB/c mice were intramuscularly vaccinated on day 1 and boosted on day 14 and 21. Serum were sampled on day 28. Vaginal lavage fluid, spleen, and Peyer's Patch were sampled on day 35 and day 42. (**b**) IgG level of serum on day 28. (**c**) and IgA level of vaginal lavage fluid on day 35. VLF: Vaginal lavage fluid. PP: Peyer's patch. One-way ANOVA with Dunnett's test (each group vs PBS). A pre-specified comparison RA-NVs vs NVs is also shown. Data are shown as mean±SD. ns, not significant, *p < 0.05, **p < 0.01, ***p < 0.001, ****p < 0.0001.

study because a pre-validated sampling workflow to promptly neutralize gastric acidity and inhibit proteases was not available; future work will incorporate validated gastric sIgA/tissue readouts and correlation analyses with protection. These robust mucosal responses highlight the essential role of RA within the nanovaccine formulation in promoting both systemic and mucosal immunity.

T Cell Proliferation and Cytokine Production

To assess cellular immune memory, splenocytes were harvested from each group on days 35 and 42 post-immunization and restimulated with antigens in vitro. RA-NVs significantly enhanced splenocyte proliferation compared to other groups (Figure 5a) indicating robust antigen-specific T cell activation. Consistent with a mucosal-type immune profile, IL-4 and IL-17A levels were markedly elevated in the RA-NVs group (Figures 5b and c), indicating a strong Th2 and Th17 polarization. In contrast, IFN-γ levels did not differ significantly between groups on day 35 and showed only a modest increase in the RA-NVs group on day 42 (Figure S4), suggesting minimal Th1 involvement. The cytokine profiling revealed a distinct Th2/Th17-biased immune response induced by RA-NVs, characterized by increased IL-4 and IL-17A but limited IFN-γ production. This pattern aligns with the known immunomodulatory properties of RA, which is known to support mucosal immunity and IgA class switching via Th2 and Th17 pathways, while exerting minimal influence on Th1 polarization. These findings highlight that RA-NVs preferentially elicit a Th2/Th17-skewed immune response, beneficial for establishing mucosal immunity and robust IgA production.

B Cell Activation in Peyer's Patches Post-Immunization

To further explore the mechanism underlying the enhanced mucosal antibody responses, immune cell populations in Peyer's Patches were characterized by flow cytometry, focusing on CD45+ leukocytes, CD45+CD19+ B cells, and CD45

https://doi.org/10.2147/IJN.S557242

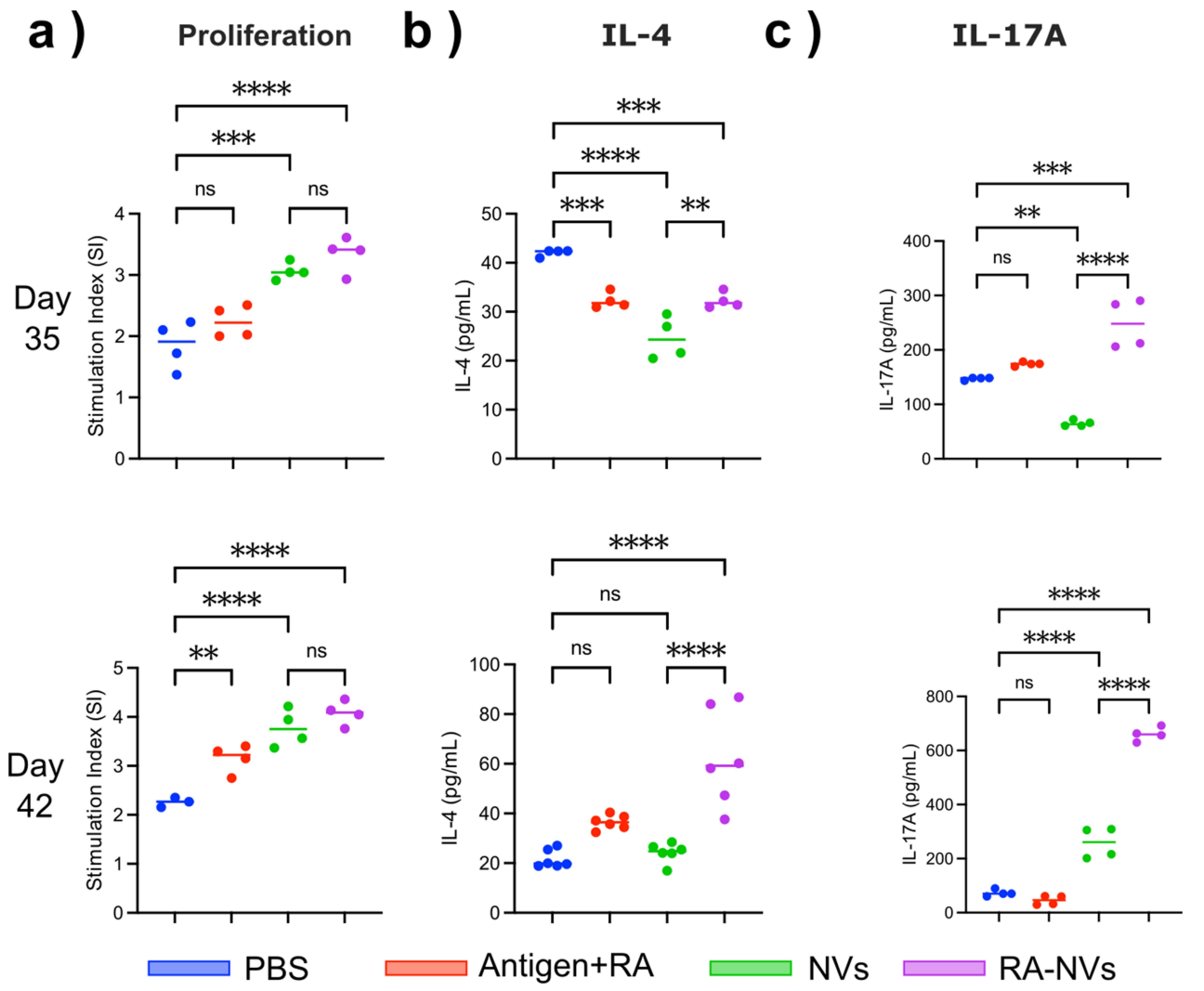

Figure 5 RA-NVs promoted antigen-specific lymphocyte proliferation and induced Th2/Th17-based cytokine responses. (**a**) Stimulation index (SI) of splenocytes on day 35 and day 42 post-immunization after in vitro antigen restimulation. (**b**) IL-4 and (**c**) IL-17A concentrations in culture supernatants measured by ELISA. For Day 35 and Day 42 analyzed separately: one-way ANOVA with Dunnett's test (each group vs PBS). The pre-specified comparison RA-NVs vs NVs is displayed on the graphs. Data are mean ± SD; n denotes biologically independent samples per group (individual points shown). Data are shown as mean±SD. *p < 0.05, **p < 0.01, ***p < 0.001, ****p < 0.0001.

+CD138+ plasma cells (Figure 6 and Figure S5). Notably, RA-NVs treatment significantly increased the proportion of CD45+CD138+ plasma cells, indicative of enhanced B-cell differentiation. These plasma cells are crucial for the production of antigen-specific antibodies, particularly secretory IgA, which neutralizes pathogens at mucosal surfaces, including the gastrointestinal tract where *f* colonizes. The increased plasma cell population thus aligns with the observed elevation of mucosal IgA levels, supporting the critical role of RA-NVs in promoting mucosal immunity.

The Protective Efficacy of the RA-NVs Against H. pylori

To demonstrate the protective efficacy of the RA-NVs vaccine, BALB/c mice were intramuscularly immunized with RA-NVs and subsequently orally challenged with mouse-adapted *H. pylori* strain J99 (Figure 7a). On day 49, mice were euthanized and bacterial colonization in gastric mucosa was assessed using quantitative bacterial culture. The vaccinated group showed significantly reduced *H. pylori* colonization compared to controls (Figure 7b), demonstrating effective immune-mediated bacterial clearance. Histological examination (H&E staining) further revealed significantly reduced gastric inflammation in RA-NVs-treated mice (Figure 7c). In contrast, non-immunized, infected mice (Blank group)

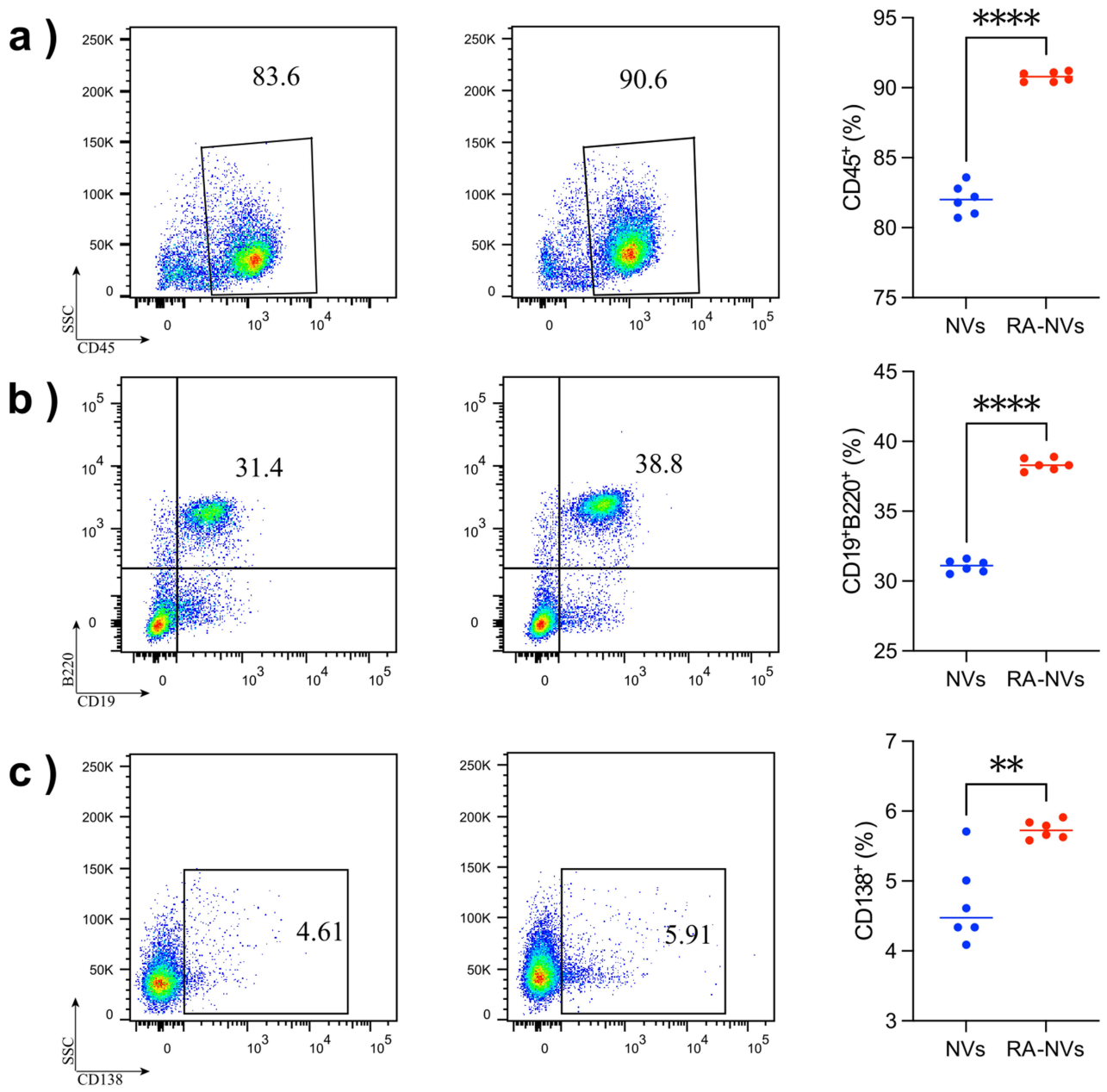

Figure 6 Percent of (**a**) CD45+, (**b**) CD45+CD19+ B cells, (**c**) CD45+CD138+ plasma cells isolated from Peyer's patch. Unpaired two-tailed *t*-test (RA-NVs vs NVs). Data are mean ± SD. ** P < 0.01; **** P < 0.0001.

exhibited signs of chronic gastritis, characterized by pronounced immune cell infiltration, including mononuclear cells and neutrophils within the submucosal region. The minimal inflammation observed in the RA-NVs group highlights a robust mucosal immune response that effectively mitigates bacterial colonization and persistence.

Biosafety and Biocompatibility Assessment

Figure 8a presents histological examination of major organs (liver, kidney, spleen, lung, and heart) from mice on day 35 after immunization with RA-NVs. The results showed no significant pathological changes in any organs. Specifically, no inflammatory infiltrates, tissue necrosis, or signs of organ damage were observed, confirming the biocompatibility and safety of RA-NVs.

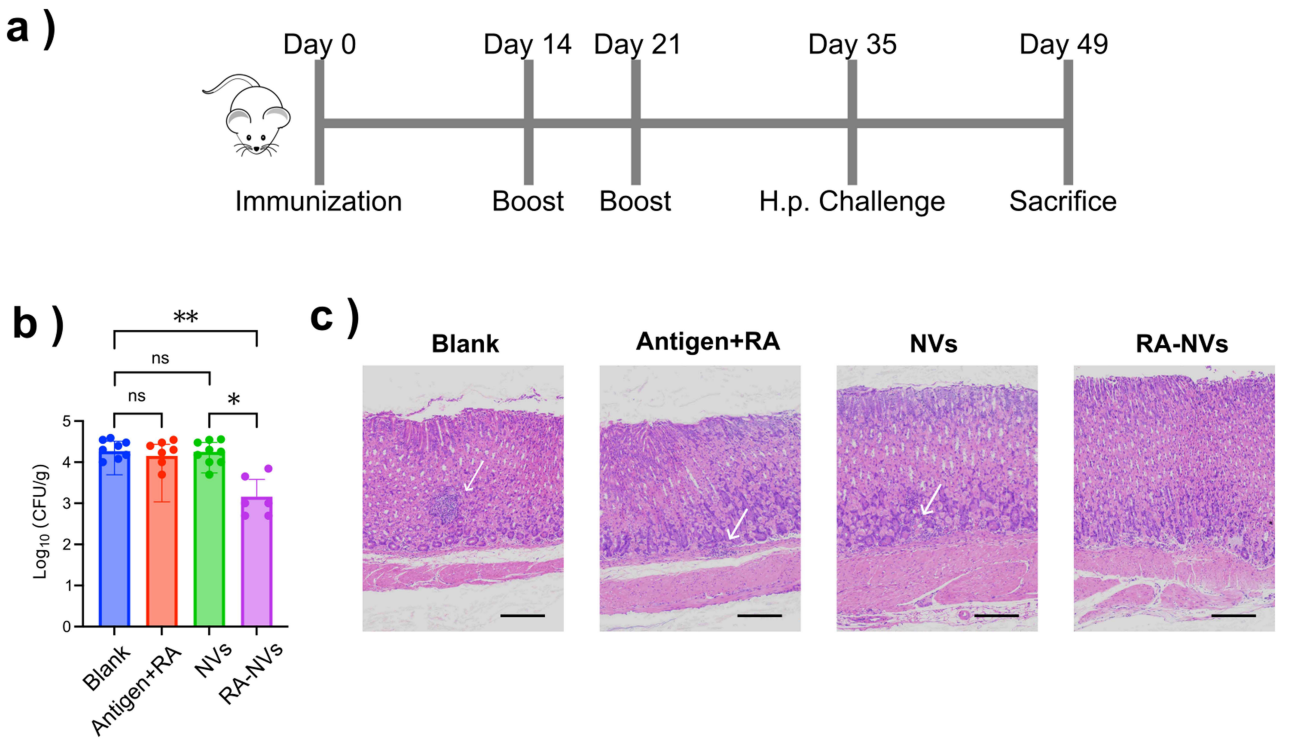

Figure 7 (**a**) Scheme of experiment. BALB/c mice were intramuscularly vaccinated on day 1 and boosted on day 14 and 21. *H. p.* bacteria were challenged on day 35. The mice were sacrificed on day 49. (**b**) The number of *H. pylori* colonizing the gastric mucosa was measured using quantitative culture. (**c**) Hematoxylin-eosin staining of gastric mucosa. Arrows indicate areas with residual inflammatory cell infiltrates. Scale bar: 10 μm. One-way ANOVA with Dunnett's test (each group vs Blank/PBS as indicated). The pre-specified comparison RA-NVs vs NVs is also shown. Data are mean ± SD. Data are shown as mean±SD. *p < 0.05, **p < 0.01.

Furthermore, the safety profile was assessed by analyzing serum biochemical parameters, including alkaline phosphatase (ALP), alanine transaminase (ALT), aspartate transaminase (AST), creatine kinase (CK), lactate dehydrogenase (LDH), uric acid (UA), urea (UREAL), and creatinine (CREA) (Figure 8b). These biomarkers reflect liver, kidney, and muscle function. All measured parameters remained within normal ranges, comparable to those in control mice, suggesting no hepatotoxicity, nephrotoxicity, or muscle damage induced by RA-NVs. These findings collectively support the safety and biocompatibility of the nanovaccine formulation.

Conclusions

In conclusion, this study highlights the efficacy of RA-NVs as a novel intramuscular nanovaccine for preventing *H. pylori* infection. Despite intramuscular injection, RA-NVs successfully induced potent mucosal and systemic immune responses, evidenced by significantly elevated IgG and IgA levels, robust T cell activation, and a Th2/Th17-skewed response. The vaccine also promoted B cell activation in Peyer's Patches, effectively reducing gastric colonization of *H. pylori*. Notably, RA-NVs exhibited excellent biosafety, demonstrating no detectable organ toxicity or adverse biochemical changes. These findings indicate that RA-NVs represent a promising strategy for mucosal pathogen vaccination via an intramuscular route. Our evaluation focused on the early post-boost window, and as an early-stage preclinical study in mice these results are hypothesis-generating. Human studies will be essential to establish safety, immunogenicity, durability, dosing, and efficacy. Future work will extend follow-up and include later time-point challenge studies to define durability and guide further optimization of the RA-NVs formulation for clinical translation. In addition, a standardized head-to-head comparison with an oral formulation using the identical antigens (UreA/UreB) is planned to directly benchmark performance and substantiate any potential advantage.

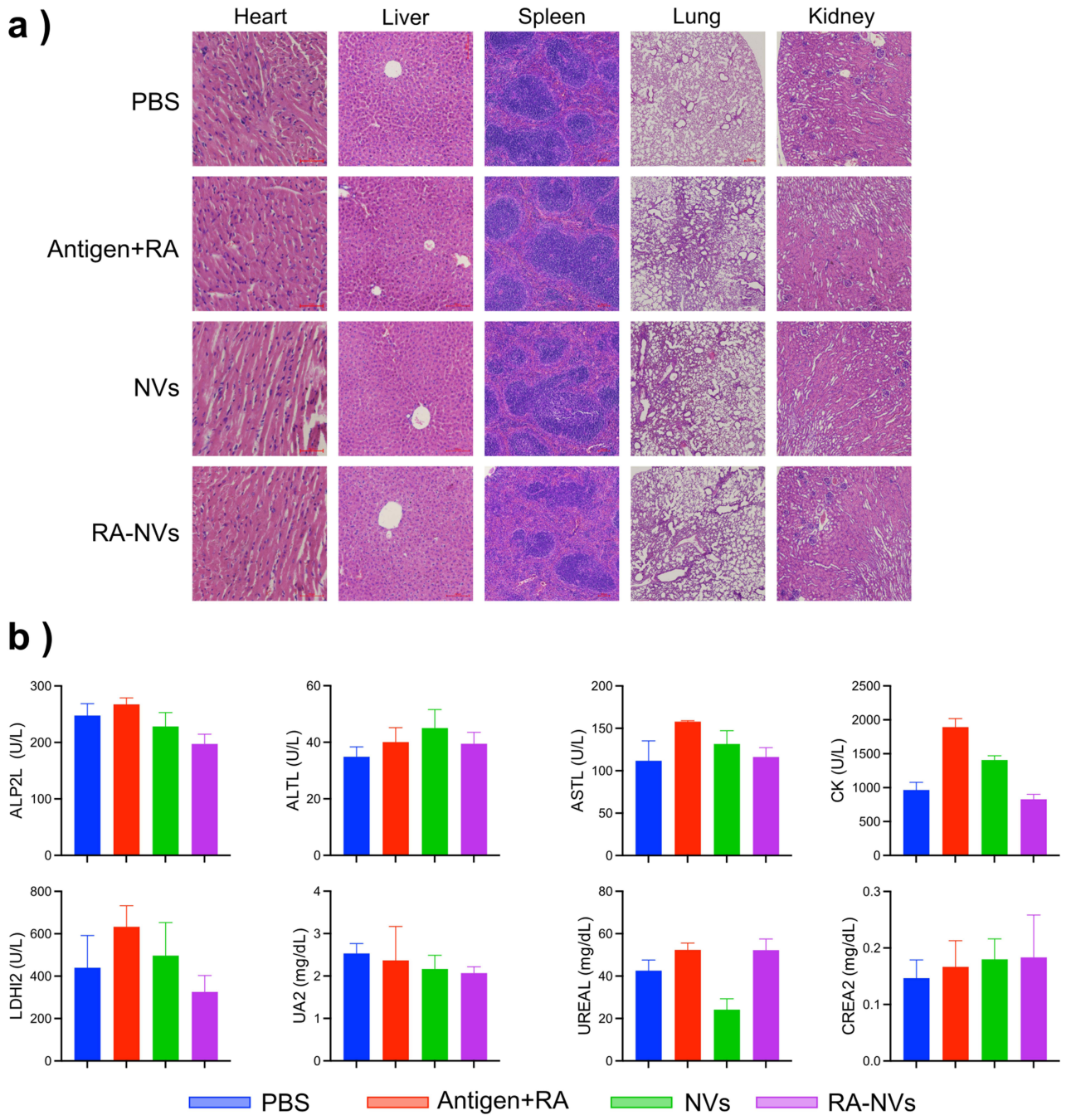

Figure 8 (**a**) Histological examination of the major organs from mice on day 35 after immunization. All images shown are of 400x magnification. (**b**) Serum biochemical parameters from mice on day 35.

Abbreviations: ALP2L, Alkaline phosphatase; ALTL, Alanine transaminase; ASTL, Aspartate Transaminase; CK, Creatine Kinase; LDHI2, lactate dehydrogenase; UA2, uric acid; UREAL, urea; CREA2, Creatinine.

Institutional Review Board Statement

All animal procedures were performed in accordance with the National Standard of the People's Republic of China GB/T 35892-2018 Laboratory animal—Guideline for ethical review of animal welfare and GB 14925-2023 Laboratory animal—Environment and housing facilities, and were approved by the Institutional Animal Care and Ethics Committee of Sichuan University (protocol No. 20220113002).

https://doi.org/10.2147/IJN.S557242

Abbreviations

APC, antigen-presenting cell; CCK-8, Cell Counting Kit-8; CCR9, C-C chemokine receptor 9; CCL25, C-C motif chemokine ligand 25; CFU, colony-forming units; Cy5-NHS, Cyanine 5 N-Hydroxysuccinimide Ester; DC, dendritic cell; *H. pylori, Helicobacter pylori*; H&E, hematoxylin and eosin; IgA/IgG, immunoglobulin A/G; IVIS, in vivo imaging system; OVA, ovalbumin; PLGA, poly(lactic-co-glycolic acid); PP(s), Peyer's patches; PVA, poly(vinyl alcohol); RA, all-trans retinoic acid; sIgA, secretory IgA; VLF(s), vaginal lavage fluid(s).

Data Sharing Statement

Data are available from the corresponding authors, Gang Guo (guogang7001@163.com) and Kaiyun Liu (liu-kaiyun@wchscu.edu.cn), upon reasonable request.

Funding

We acknowledge financial support from the National Natural Science Foundation of China (Grant Nos. 32200768), Natural Science Foundation of Sichuan Province (Grant Nos 2024NSFSC8131), and 1.3.5 Project for Disciplines of Excellence, West China Hospital, Sichuan University, project Grants ZYXY21003.

Disclosure

The authors declare no conflicts of interest.

References

1. Turner JR. Intestinal mucosal barrier function in health and disease. *Nat Rev Immunol*. 2009;9(11):799–809. doi:10.1038/nri2653
2. Wang Z, Cui K, Costabel U, Zhang X. Nanotechnology-facilitated vaccine development during the coronavirus disease 2019 (COVID-19) pandemic. *Exploration*. 2022;2(5):20210082. doi:10.1002/EXP.20210082
3. Lavelle EC, Ward RW. Mucosal vaccines — fortifying the frontiers. *Nat Rev Immunol*. 2022;22(4):236–250. doi:10.1038/s41577-021-00583-2
4. Malfertheiner P, Camargo MC, El-Omar E, et al. Helicobacter pylori infection. *Nat Rev Dis Primers*. 2023;9(1):19. doi:10.1038/s41572-023-00431-8
5. Magalhães Queiroz DM, Luzza F. Epidemiology of Helicobacter pylori Infection. *Helicobacter*. 2006;11(s1):1–5. doi:10.1111/j.1478-405X.2006.00429.x
6. Malfertheiner P, Megraud F, O'Morain CA, et al. Management of Helicobacter pylori infection-the Maastricht V/Florence consensus report. *Gut*. 2017;66(1):6–30. doi:10.1136/gutjnl-2016-312288
7. Czinn SJ, Blanchard T. Vaccinating against Helicobacter pylori infection. *Nat Rev Gastroenterol Hepatol*. 2011;8(3):133–140. doi:10.1038/nrgastro.2011.1
8. Zeng M, Mao XH, Li JX, et al. Efficacy, safety, and immunogenicity of an oral recombinant Helicobacter pylori vaccine in children in China: a randomised, double-blind, placebo-controlled, Phase 3 trial. *Lancet*. 2015;386(10002):1457–1464. doi:10.1016/S0140-6736(15)60310-5
9. Vela Ramirez JE, Sharpe LA, Peppas NA. Peppas, Current state and challenges in developing oral vaccines. *Adv Drug Delivery Rev*. 2017;114:116–131. doi:10.1016/j.addr.2017.04.008
10. Larange A, Cheroutre H. Retinoic acid and retinoic acid receptors as pleiotropic modulators of the immune system. *Ann Rev Immunol*. 2016;34 (Volume 34, 2016):369–394. doi:10.1146/annurev-immunol-041015-055427
11. Liu Z-M, Wang K-P, Ma J, Guo Zheng S. The role of all-trans retinoic acid in the biology of Foxp3+ regulatory T cells. *Cell Mol Immunol*. 2015;12 (5):553–557. doi:10.1038/cmi.2014.133
12. Iwata M, Hirakiyama A, Eshima Y, Kagechika H, Kato C, Song S-Y. Retinoic acid imprints gut-homing specificity on T cells. *Immunity*. 2004;21 (4):527–538. doi:10.1016/j.immuni.2004.08.011
13. Christensen D, Bøllehuus Hansen L, Leboux R, et al. A liposome-based adjuvant containing two delivery systems with the ability to induce mucosal immunoglobulin a following a parenteral immunization. *ACS Nano*. 2019;13(2):1116–1126. doi:10.1021/acsnano.8b05209
14. Du Y, Xia Y, Zou Y, et al. Exploiting the lymph-node-amplifying effect for potent systemic and gastrointestinal immune responses via polymer/lipid nanoparticles. *ACS Nano*. 2019;13(12):13809–13817. doi:10.1021/acsnano.9b04071
15. Li W, Li Y, Li J, et al. All-trans-retinoic acid-adjuvanted mRNA vaccine induces mucosal anti-tumor immune responses for treating colorectal cancer. *Adv Sci*. 2024;11(22):2309770. doi:10.1002/advs.202309770
16. Zhong X, Du G, Wang X, et al. Nanovaccines mediated subcutis-to-intestine cascade for improved protection against intestinal infections. *Small*. 2022;18(1):2105530. doi:10.1002/smll.202105530
17. Xia Y, Wu J, Du Y, Miao C, Su Z, Ma G. Bridging systemic immunity with gastrointestinal immune responses via oil-in-polymer capsules. *Adv Mater*. 2018;30(31):1801067. doi:10.1002/adma.201801067
18. Hu LT, Mobley HL. Purification and N-terminal analysis of urease from Helicobacter pylori. *Infect Immun*. 1990;58(4):992–998. doi:10.1128/iai.58.4.992-998.1990
19. Blanchard TG, Czinn SJ. Identification of Helicobacter pylori and the evolution of an efficacious childhood vaccine to protect against gastritis and peptic ulcer disease. *Pediatr Res*. 2017;81(1–2):170–176. doi:10.1038/pr.2016.199
20. Zhong Y, Chen J, Liu Y, et al. Oral immunization of BALB/c mice with recombinant Helicobacter pylori antigens and double mutant heat-labile toxin (dmLT) induces prophylactic protective immunity against *H. pylori* infection. *Microb Pathogenesis*. 2020;145:104229. doi:10.1016/j.micpath.2020.104229

21. McCall RL, Sirianni RW. PLGA nanoparticles formed by single- or double-emulsion with vitamin E-TPGS. *JoVE*. 2013;82:e51015.
22. Chopra A, Willmore WG, Biggar KK. Protein quantification and visualization via ultraviolet-dependent labeling with 2,2,2-trichloroethanol. *Sci Rep*. 2019;9(1):13923. doi:10.1038/s41598-019-50385-9
23. Sauter M, Sauter RJ, Nording H, Olbrich M, Emschermann F, Langer HF. Protocol to isolate and analyze mouse bone marrow derived dendritic cells (BMDC. *STAR Protocols*. 2022;3(3):101664. doi:10.1016/j.xpro.2022.101664
24. Rhee I, Zhong M-C, Reizis B, Cheong C, Veillette A. Control of dendritic cell migration, T cell-dependent immunity, and autoimmunity by protein tyrosine phosphatase PTPN12 expressed in dendritic cells. *Mol Cell Biol*. 2014;34(5):888–899. doi:10.1128/MCB.01369-13
25. Justus CR, Marie MA, Sanderlin EJ, Yang LV. Transwell in vitro cell migration and invasion assays. *Methods Mol Biol*. 2023;2644:349–359.
26. Guo L, Liu K, Xu G, et al. Prophylactic and therapeutic efficacy of the epitope vaccine CTB-UA against Helicobacter pylori infection in a BALB/c mice model. *Appl Microbiol Biotechnol*. 2012;95(6):1437–1444. doi:10.1007/s00253-012-4122-0
27. Gossmann R, Spek S, Langer K, Mulac D. Didodecyldimethylammonium bromide (DMAB) stabilized poly(lactic-co-glycolic acid) (PLGA) nanoparticles: uptake and cytotoxic potential in Caco-2 cells. *J Drug Delivery Sci Technol*. 2018;43:430–438. doi:10.1016/j.jddst.2017.11.002
28. Svensson M, Johansson-Lindbom B, Zapata F, et al. Retinoic acid receptor signaling levels and antigen dose regulate gut homing receptor expression on CD8 + T cells. *Mucosal Immunol*. 2008;1(1):38–48. doi:10.1038/mi.2007.4
29. Mora JR, Iwata M, Eksteen B, et al. Generation of gut-homing IgA-secreting B cells by intestinal dendritic cells. *Science*. 2006;314 (5802):1157–1160. doi:10.1126/science.1132742
30. Kim MH, Taparowsky EJ, Kim CH. Retinoic acid differentially regulates the migration of innate lymphoid cell subsets to the gut. *Immunity*. 2015;43(1):107–119. doi:10.1016/j.immuni.2015.06.009